Biomedical Optics EXPRESS

Optically trapping tumor cells to assess differentiation and prognosis of cancers

M. Pradhan,[1] S. Pathak,[1] D. Mathur,[2,4] and U. Ladiwala[1,3]

[1]*UM-DAE Centre for Excellence in Basic Sciences, Kalina Campus, Mumbai 400 098, India*
[2]*Tata Institute of Fundamental Research, 1 Homi Bhabha Road, Mumbai 400 005, India*
[3]*brainwave.surf@gmail.com*
[4]*atmol1@tifr.res.in*

Abstract: We report an optical trapping method that may enable assessment of the differentiation status of cancerous cells by determining the minimum time required for cell-cell adhesion to occur. A single, live cell is trapped and brought into close proximity of another; the minimum contact time required for cell-cell adhesion to occur is measured using transformed cells from neural tumor cell lines: the human neuroblastoma SK-N-SH and rat C6 glioma cells. Earlier work on live adult rat hippocampal neural progenitors/stem cells had shown that a contact minimum of ~5 s was required for cells to adhere to each other. We now find the average minimum time for adhesion of cells from both tumor cell lines to substantially increase to ~20-25 s, in some cases up to 45 s. Upon in vitro differentiation of these cells with all-trans retinoic acid the average minimum time reverts to ~5-7 s. This proof-of-concept study indicates that optical trapping may be a quick, sensitive, and specific method for determining differentiation status and, thereby, the prognosis of cancer cells.

OCIS codes: (170.1530) Cell analysis; (000.1430) Biology and medicine.

References and links

1. A. A. Kornyshev, "From biologically-inspired physics to physics-inspired biology," J. Phys. Condens. Matter **22**(41), 410401 (2010).
2. M. Gruebele and D. Thirumalai, "Perspective: Reaches of chemical physics in biology," J. Chem. Phys. **139**(12), 121701 (2013).
3. D. Mathur, "Biology-inspired AMO physics," J. Phys. B **48**(2), 022001 (2015).
4. Y. Sung, N. Lue, B. Hamza, J. Martel, D. Irimia, R. R. Dasari, W. Choi, Z. Yaqoob, and P. So, "Three-dimensional holographic refractive-index measurement of continuously flowing cells in a microfluidic channel," Phys. Rev. Appl. **1**(1), 014002 (2014).
5. S. E. Cross, Y. S. Jin, J. Rao, and J. K. Gimzewski, "Nanomechanical analysis of cells from cancer patients," Nat. Nanotechnol. **2**(12), 780–783 (2007).
6. P. Katira, M. H. Zaman, and R. T. Bonnecaze, "How changes in cell mechanical properties induce cancerous behavior," Phys. Rev. Lett. **108**(2), 028103 (2012).
7. R. E. Mahaffy, C. K. Shih, F. C. MacKintosh, and J. Käs, "Scanning probe-based frequency-dependent microrheology of polymer gels and biological cells," Phys. Rev. Lett. **85**(4), 880–883 (2000).
8. F. Wottawah, S. Schinkinger, B. Lincoln, R. Ananthakrishnan, M. Romeyke, J. Guck, and J. Käs, "Optical rheology of biological cells," Phys. Rev. Lett. **94**(9), 098103 (2005).
9. U. Ladiwala, H. Basu, and D. Mathur, "Assembling neurospheres: dynamics of neural progenitor/stem cell aggregation probed using an optical trap," PLoS One **7**(6), e38613 (2012).
10. H. Mori, T. Fujitani, Y. Kanemura, M. Kino-Oka, and M. Taya, "Observational examination of aggregation and migration during early phase of neurosphere culture of mouse neural stem cells," J. Biosci. Bioeng. **104**(3), 231–234 (2007).
11. A. Jögi, M. Vaapil, M. Johansson, and S. Pahlman, "Cancer cell differentiation heterogeneity and aggressive behavior in solid tumors," Ups. J. Med. Sci. **117**(2), 217–224 (2012).
12. S. Joshi, R. Guleria, J. Pan, D. DiPette, and U. S. Singh, "Retinoic acid receptors and tissue-transglutaminase mediate short-term effect of retinoic acid on migration and invasion of neuroblastoma SH-SY5Y cells," Oncogene **25**(2), 240–247 (2006).
13. B. Campos, F. Wan, M. Farhadi, A. Ernst, F. Zeppernick, K. E. Tagscherer, R. Ahmadi, J. Lohr, C. Dictus, G. Gdynia, S. E. Combs, V. Goidts, B. M. Helmke, V. Eckstein, W. Roth, P. Beckhove, P. Lichter, A. Unterberg, B.

#257425 Received 13 Jan 2016; revised 16 Feb 2016; accepted 16 Feb 2016; published 19 Feb 2016

Radlwimmer, and C. Herold-Mende, "Differentiation therapy exerts antitumor effects on stem-like glioma cells," Clin. Cancer Res. **16**(10), 2715–2728 (2010).
14. K. Bambardekar, A. K. Dharmadhikari, J. A. Dharmadhikari, D. Mathur, and S. Sharma, "Measuring erythrocyte deformability with fluorescence, fluid forces, and optical trapping," J. Biomed. Opt. **13**(6), 064021 (2008).
15. P. Kumari, J. A. Dharmadhikari, A. K. Dharmadhikari, H. Basu, S. Sharma, and D. Mathur, "Optical trapping in an absorbing medium: from optical tweezing to thermal tweezing," Opt. Express **20**(4), 4645–4652 (2012).
16. J. D. Walton, D. R. Kattan, S. K. Thomas, B. A. Spengler, H.-F. Guo, J. L. Biedler, N.-K. V. Cheung, and R. A. Ross, "Characteristics of Stem Cells from Human Neuroblastoma Cell Lines and in Tumors," Neoplasia **6**(6), 838–845 (2004).
17. C. S. Niu, M. W. Li, Y. F. Ni, J. M. Chen, J. M. Mei, J. Li, and X. M. Fu, "Effect of all-trans retinoic acid on the proliferation and differentiation of brain tumor stem cells," J. Exp. Clin. Cancer Res. **29**(1), 113–121 (2010).
18. V. P. Chekhonin, V. P. Baklaushev, G. M. Yusubalieva, K. A. Pavlov, O. V. Ukhova, and O. I. Gurina, "Modeling and immunohistochemical analysis of C6 glioma in vivo," Bull. Exp. Biol. Med. **143**(4), 501–509 (2007).
19. P. N. Preis, H. Saya, L. Nádasdi, G. Hochhaus, V. Levin, and W. Sadée, "Neuronal cell differentiation of human neuroblastoma cells by retinoic acid plus herbimycin A," Cancer Res. **48**(22), 6530–6534 (1988).
20. N. Pouliot, H. B. Pearson, and A. Burrows, "Investigating metastasis using in vitro platforms" in Metastatic Cancer: Clinical and Biological Perspectives, Rahul Jandial (ed) (Landes Bioscience, 2013).
21. J. A. Ludwig and J. N. Weinstein, "Biomarkers in cancer staging, prognosis and treatment selection," Nat. Rev. Cancer **5**(11), 845–856 (2005).
22. S. Domcke, R. Sinha, D. A. Levine, C. Sander, and N. Schultz, "Evaluating cell lines as tumour models by comparison of genomic profiles," Nat. Commun. **4**, 2126–2136 (2013).

1. Introduction

The manner in which contemporary biology is beginning to be significantly influenced by physics has been highlighted in several cogent reviews (see [1–3] and references therein). Optical methods that go beyond microscope-based imaging methods continue to drive developments [4]. The initial manifestation of such techniques involved optical traps probing how mechanical stress can regulate cellular processes. Trapping has permitted observation of differences in the mechanical properties of healthy and cancerous cells [5], relevant to the proliferation of cancerous cells [6]. Normal and cancerous endothelial cells exhibit differing values of Young's modulus [7]. Optical stretching of healthy and malignantly transformed fibroblast cells show differences in "stretchability" [8]. Recently, optical trapping has probed the mechanics and spatio-temporal dynamics of how neural stem cells (NSCs) adhere and aggregate [9] to show that cell-cell adhesion dynamics occur on seconds timescales: two NSCs need to be close to each other for a minimum mean time of ~5 s for adhesion to occur, or before a single NSC adheres to a neurosphere – an aggregate of NSCs. Incorporation of fluid flow methods into the optical trap [9] enabled quantification of a lower limit of ~18 pN as the adhesive force required by proximate NSCs. Prior to the use of a trap, such studies had relied on time-lapse microscopy which accessed only longer timescales (0.5-3 hours) [10].

We report here a proof-of-concept study that uses trapping to assess the differentiation status of tumor cells and, thereby, the prognosis of cancers. The differentiation status of a cancer helps classify solid tumors into various grades, from poor to well-differentiated. It indicates tumor aggressiveness and is, hence, of prognostic significance. Biologically, differentiation applies to the developmental process whereby a cell - originating from the quintessential stem cell - acquires functional specialization. Developmentally, differentiation is irreversible but, in the context of cancer, differentiation can reverse: cells can "de-differentiate" with the extent of de-differentiation determining the behavior of the tumor. A poorly differentiated tumor would be more aggressive and have a worse prognosis than its well-differentiated counterpart. A high degree of differentiation means that the tumor has greater structural similarity to its tissue of origin; at low stages of differentiation almost all structural similarity is lost: the cells display reduced cohesiveness and increased invasiveness into surrounding tissues and to distant organs, forming secondary metastatic tumors [11].

Our probing of cancerous cell differentiation relies on quantifying differences in the time taken for cell-cell adhesion of chemically differentiated and undifferentiated single, live malignant cells from two established neural tumor cell lines: the human neuroblastoma SK-N-SH and rat C6 glioma cells. We show that assessment of minimum cell-cell adhesion time is a

#257425 Received 13 Jan 2016; revised 16 Feb 2016; accepted 16 Feb 2016; published 19 Feb 2016

label-free, fairly sensitive, specific, reproducible, rapid, and fairly accurate signature of the differentiation status and prognosis of malignant cells.

2. Experimental methods

2.1. Cell culture

C6 glioma and SK-NSH neuroblastoma cell lines were cultured in DMEM supplemented with 10% FBS, 50 μg/ml penicillin, streptomycin and 2mM glutamine (Invitrogen, USA) and maintained in CO_2 at 37 C. Cells were passaged when plates were nearly confluent. We chemically induced differentiation using all-trans retinoic acid (ATRA), a strong inducer of differentiation in various cell lines and tumors, including neuroblastomas and gliomas [12,13]. Cells of both cancerous lines could be differentiated to a better grade (assessed by us using immunofluorescence staining and microscopy) with a final concentration of 20 ng/ml of ATRA (Sigma Aldrich, USA). ATRA was dissolved in DMSO, and added to differentiation medium comprising the above medium but with 2% FBS, on alternate days for a period of 13 days for C6 glioma cells and 8/13 days for SK-N-SH cells.

2.2. Optical trap

Our optical trap has been described before [14,15, and references therein]. Briefly, the set-up (Fig. 1) comprised a 1 W Nd:YVO_4 laser producing a 2 mm diameter beam of 1064 nm light which was expanded to 8 mm and coupled to an inverted microscope. Trapping was achieved by tight focusing of this light with a 100X oil-immersed objective (NA = 1.3). A beam profiler measured the focused spot to be 0.6-1 μm in diameter, much smaller than cell diameters (6-10 μm). The very small laser-cell interaction volume was near the cell center, well away from the periphery where the hitherto-unknown biochemistry of adhesion occurs. Nevertheless, the entire cell was optically trapped and not just some organelle within it, as surmised from measurements made on a trapped cell subjected to a fluid force. At sufficiently large forces the cell escaped the trap; at lower values it essentially retained its shape. The trapped cells were imaged through the same objective by a CCD camera. The laser power was measured with an integrating sphere (located after the objective) and a calibrated photodiode.

Our experiments were performed using powers (P) in the 5-50 mW range. At P<5 mW negligible trapping occurred; we avoided values of P>50 mW to minimize the possibility of cell damage [14]. Most results were obtained at ~15 mW. By correlating P with the optical force generated [9], we deduced that a trapped cell experienced a force of 10 ± 2 pN, using Stoke's Law to estimate the minimum fluid velocity required to displace it from within the trap. The force is an estimate because drag coefficients are unknown for cell shapes used in our experiments. We also determined trapping force by monitoring the Brownian motion of a trapped cell on a quadrant photodiode, measuring the power spectrum and, from it, deducing a value for the trap stiffness [15]. The two types of measurements yielded trap stiffness values that were mutually consistent to ± 50%.

2.3. Trapping procedure and statistical analysis

ATRA-treated or untreated cells were aspirated, centrifuged at 1000 rpm, washed with 1x PBS and re-suspended to a cell density of $5x10^5$ cells/ml. Single cell suspensions were made by pipetting and vortexing; 20 μl of the suspension was loaded on a square 22 mm acid-cleaned glass coverslip attached to a translation stage. A single cell was randomly selected from within the microscope's field of view; it was trapped and brought in close proximity to another cell for increasing amounts of time before the trapped cell was "pulled" away so as to determine whether adhesion had occurred or not (Fig. 2(a), 2(b)). The minimum time, $\tau_{min,}$ needed for the cells to adhere to each other was determined from individual movie frames. τ_{min} depends, of course, on P; we used P-values that yielded a constant trapping force of ~10 pN and, therefore, different groups of our data are comparable. On average, at least 20 cells per measurement were studied; histograms yielded a distribution of τ_{min} values. We confirmed that these histograms were qualitatively independent of P. Statistical significance was

#257425 Received 13 Jan 2016; revised 16 Feb 2016; accepted 16 Feb 2016; published 19 Feb 2016

calculated using non-parametric tests (one way ANOVA with post-hoc Tukey-Kramer tests); p values ≤ 0.05 were considered significant.

2.4. Immunofluorescence staining and microscopy

Immunofluorescence staining of treated and untreated cells helped assess the differentiation of ATRA-treated cancerous cells. C6 glioma and SK-N-SH cells were seeded on coverslips in 12-well plates (~1000 cells/coverslip). On the following day, the cells were differentiated using the above-mentioned protocol. Cells were then washed with PBS, fixed with 4% para-formaldehyde for 15 minutes (25 C) and permeabilized with 0.3% triton X-100.

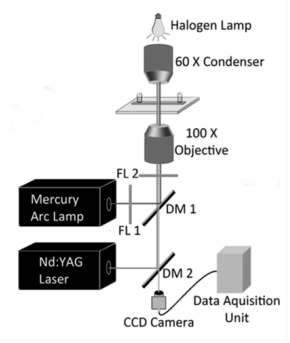

Fig. 1. Schematic diagram of our optical trap (see text). Cell trapping occurred on the microscope slide placed after the oil-immersed 100X objective. DM: dichroic mirrors, FL: filters.

Cells were incubated with primary antibodies, mouse anti-GFAP and rabbit anti-β-tubulin III, with blocking using 5% horse serum. Secondary antibodies labelled with Alexa fluor 488 were incubated with cells for 1 hour. Washed cells were counterstained with nuclear stain Hoechst for 10 minutes; a Nikon 90i fluorescence microscope was used for imaging.

3. Results and discussion

Measured histograms of τ_{min} values were found to depend on the cells' differentiation status, that is, on whether they were untreated or ATRA-differentiated. As noted, we optically trapped a randomly selected, single, live cell and brought it in close proximity to another cell. Through a series of measurements (see real-time movie clips) we assessed τ_{min} for different cells (Fig. 2(c), 2(d)) and discovered that they were significantly longer for untreated cells of both cell lines tested (12-44 s, with a mean of 27 s for SK-N-SH cells; 9-36 s, with a mean of 21 s for C6 glioma cells) than that for normal NSCs (~5 s) [9]. ATRA treatment induced dramatic reduction of τ_{min} for all cells from both cell lines, with a minimum time of 4 s and an upper limit of 16 s (Fig. 2(c), 2(d)). Untreated SK-N-SH cells (n = 16) showed a bimodal distribution of τ_{min} values, with a peak of 25% cells at 25-28 s and another 20% of cells at 37-40 s (Fig. 2(c)); this variation is most likely due to cellular heterogeneity, a prominent feature of neuroblastomas [16]. Upon ATRA treatment of SK-N-SH cells (n = 25), τ_{min} of all cells reduced substantially: 4-16 s (mean = 9 s). The majority of cells (48%) had τ_{min} in the lowest time interval of 5-8 s (Fig. 2(c)). τ_{min} for untreated C6 glioma cells (n = 22) covered the range 9-36 s (mean = 21 s). Upon ATRA treatment (n = 26), the time range was 5-14 s (mean = 8 s). 60% of these cells had a minimum cell-cell adhesion time between 5 and 8 s (Fig. 2(d)). For both cell lines, τ_{min} for untreated and ATRA-treated cells showed an overlap between 9 and 16 s. Of the total of 41 observations for SK-N-SH cells, 13 ATRA-treated cells and 14 untreated cells were correctly discriminated by our method. 12 ATRA-treated cells were incorrectly classified as undifferentiated and 2 untreated cells as differentiated, indicating 52% sensitivity and 87.5% specificity for SK-N-SH cells. Of 49 observations on C6 glioma cells, 16 ATRA- treated cells and 16 untreated cells were correctly discriminated. 11 ATRA-

#257425 Received 13 Jan 2016; revised 16 Feb 2016; accepted 16 Feb 2016; published 19 Feb 2016

treated cells were incorrectly classified as undifferentiated and 6 untreated cells as differentiated, indicating 59% sensitivity and 72% specificity for C6 glioma cells.

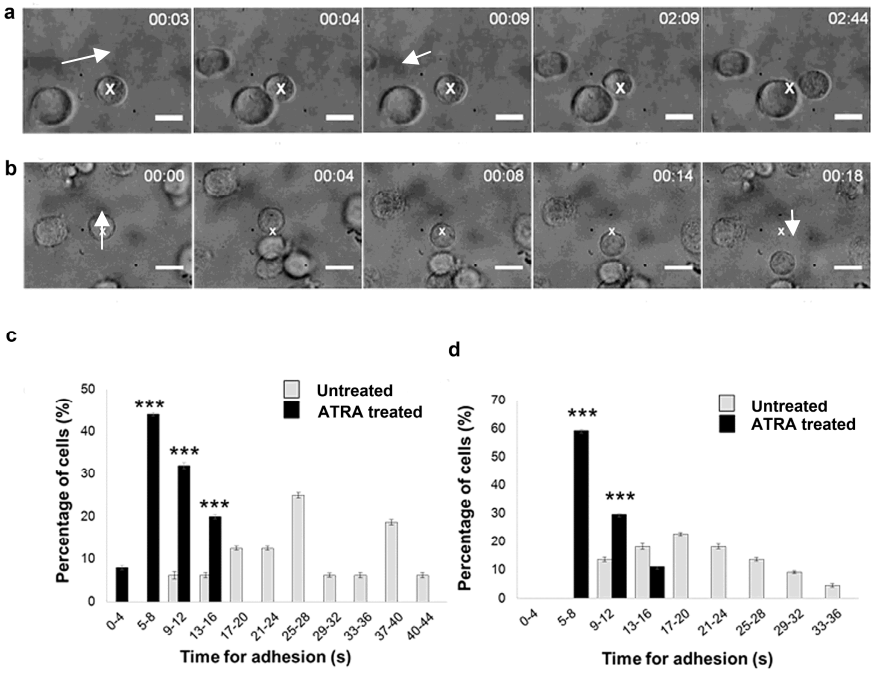

Fig. 2. Dependence of minimum time for cell-cell adhesion on differentiation status of malignant cells. Time lapse images from real time movies depicting (a) an untreated C6 glioma cell made to approach another (Visualization 1). The trap is moved after every (n + 5) second where n = 0, 5, 10, 15 s. Cells were allowed to remain in contact till they could not be pulled apart by the trap: the time taken was designated the minimum time for cell-cell adhesion. The white cross denotes the trapped cell. In the first three frames, another cell is made to approach the trapped cell in the direction of the arrow. As the trap is moved away after 9 s, the cells are seen to separate. Eventually, the cells remain adhered to each other (last two frames). (b) Similar time lapse images from real-time movies for ATRA-treated C6 glioma cells showing adherence after 4 s contact (Visualization 2). (c), (d) Percentage of undifferentiated and ATRA-treated cells undergoing irreversible cell adhesion at different time points (see text). (c) SK-N-SH cells; (d) C6 glioma cells. *** denotes statistical significance where $p<0.001$ for adhesion times of untreated and ATRA-treated cells.

We used immunofluorescence staining to confirm the differentiation status of cells; Figs. 3(a), 3(b) show, respectively, typical bright-field microscope images of untreated and ATRA-treated of C6 glioma cells. The former appear spindle shaped whereas the latter have smaller rounded cell bodies with spiky, elongated cytoplasmic extensions that are morphological signatures of differentiation. Upon staining for GFAP expression, some of the untreated cells show a very low intensity expression (faint green in Fig. 3(c)); most ATRA-treated cells show either high- or moderate-intensity expression (Fig. 3(d)), the intensity being correlated with levels of GFAP expression. Basal GFAP expression, which characterizes gliomas [17] and the C6 glioma cell line [18], increases in frequency and intensity upon ATRA treatment. Similarly, untreated SK-N-SH cells were spindly shaped (Fig. 3(e)) while, upon ATRA treatment, they tended to develop long, spiny, sometimes branched cytoplasmic extensions (Fig. 3(f)).

Upon staining for β-tubulin III expression - a marker for immature neurons - almost all untreated cells showed very low levels of this marker (Fig. 3(g)) whereas ATRA-treated cells showed mostly high-intensity staining (green in Fig. 3(h)). Quantitatively, 37% of ATRA-treated C6 glioma cells and ~60% of SK-N-SH cells showed very intense staining of cell bodies and processes with GFAP and β-tubulin III, respectively.

#257425 Received 13 Jan 2016; revised 16 Feb 2016; accepted 16 Feb 2016; published 19 Feb 2016

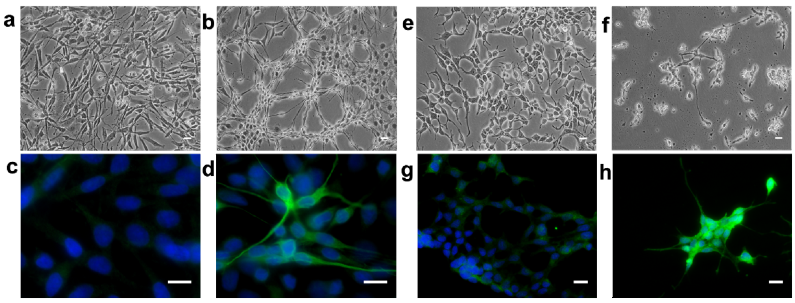

Fig. 3. Bright-field microscopy images of (a) untreated and (b) ATRA-treated C6 glioma cells, and of (e) untreated and (f) ATRA-treated SK-N-SH neuroblastoma cells. Expression of GFAP in untreated C6 cells (c) and in ATRA-treated C6 cells (d). Expression of β-tubulin III in undifferentiated SK-N-SH cells (g) showing low expression in a few cells and in ATRA-treated SK-N-SH cells (h) with moderate or intense expression in most cells. The white scale bar denotes 10 μm.

Characterizing the dynamics of the adhesion process and/or the adhesion molecular signature is expected to indicate the differentiation stage of a tumor and its propensity for metastasis. Our trap-based method shows that τ_{min} increases for all untreated malignant cells of both cell lines (mean 27 s and 21 s, respectively) - well over that for normal NSCs (~5 s) [9]. The sensitivity (52-59%) and specificity (72-87.5%) of our cell adhesion assay points to advantages over conventional methods. We note that the measured range of τ_{min} for untreated malignant cells is rather wide, a reflection of cellular heterogeneity that is a feature of cancerous tumors and cell lines, particularly neuroblastomas [11, 16] which are composed of neuroblastic and non-neuronal phenotypes [11, 19], thus also accounting for the inconstant response of the cells to differentiation with ATRA [19]. This, as well as variability in cell size and contact areas on adhesion, could influence the sensitivity of our assay; further study is needed. The overall decrease in τ_{min} for ATRA-treated cells from both cell lines (mean 9 s and 8 s, respectively) is close to the 5 s standard for normal NSCs. Although for the majority of differentiated cells (48% and 60%, respectively) $4s<\tau_{min}<8s$, the remaining time values extended only up to 16 s and never beyond, for all differentiated cells tested. The observed τ_{min} distribution could constitute a marked advantage of our method over conventional methods that usually require a plethora of reagents and longer processing time to detect differentiation; in some instances, varying stages of differentiation may even lack intermediate stage markers.

It is beyond the scope of this study to compare our method with other assays for adhesion and migration of cells, proteomics and genomics for biomarkers, isolation and detection of circulating tumor cells (see [20], and references therein). Most of these methods, used for drug sensitivity testing and for predicting metastasis, remain in the early phases of development and lack standardization [20,21]. However, in comparison to common histopathological diagnosis, which is inherently subjective, and expression of differentiation markers, ours is a more objective, quantitative, rapid, and label-free functional technique that involves simple optical instrumentation. We present this as an optics-based proof-of-concept study, having used live, single, randomly selected cells from established cancerous cell lines that have frequently found utility as *in vitro* tumor models [22]. Our method is not a pathological diagnostic; it is a simple monitor of changes in differentiation status. Further confirmatory studies with cells obtained from tumors of varying differentiation status by fine needle aspiration biopsy may be performed using our optical technique.

Acknowledgments

We are grateful to Drs. Aarti Juvekar (ACTREC, Mumbai) and Yasmin Khan (Sophia College, Mumbai) for the kind gifts of the SK-N-SH neuroblastoma and C6 glioma cell lines, respectively; we thank Sadhana Kannan (ACTREC, Mumbai) for helpful statistical inputs.

#257425 Received 13 Jan 2016; revised 16 Feb 2016; accepted 16 Feb 2016; published 19 Feb 2016